2011 American Control Conference
on O'Farrell Street, San Francisco, CA, USA
June 29 - July 01, 2011

Control of Exhaust Recompression HCCI using Hybrid Model Predictive Control

Anders Widd, Hsien-Hsin Liao, J. Christian Gerdes, Per Tunestål, and Rolf Johansson

Abstract— **Homogeneous Charge Compression Ignition (HCCI) holds promise for reduced emissions and increased efficiency compared to conventional internal combustion engines. As HCCI lacks direct actuation over the combustion phasing, much work has been devoted to designing controllers capable of set-point tracking and disturbance rejection. This paper presents results on model predictive control (MPC) of the combustion phasing in an HCCI engine based on a hybrid model formulation composed of several linearizations of a physics-based nonlinear model. The explicit representation of the MPC was implemented experimentally and the performance during set point changes was compared to that of a switched state feedback controller. The hybrid MPC produced smoother transients without overshoot when the set point change traversed several linearizations.**

I. INTRODUCTION

Homogeneous Charge Compression Ignition (HCCI), also referred to as Controlled Auto-Ignition (CAI), holds promise for reduced emissions of nitrogen oxides and increased efficiency compared to conventional internal combustion engines. The working principle of HCCI is to control the auto-ignition of a pre-mixed charge of fuel and air. This means that HCCI lacks direct actuation over the combustion phasing, making combustion phasing control a challenging control problem. Ignition timing in HCCI engines is determined by several factors including the auto-ignition properties of the air-fuel mixture, the intake temperature, and the amount of residual gases in the cylinder [1]. As a consequence, there are many possible choices of control signals, such as variable inlet and exhaust valve timing, intake temperature, etc. This work is focused on exhaust recompression HCCI, meaning that the exhaust valve is closed early so that parts of the exhausts are trapped in the cylinder. This generates an increase in charge temperature at the start of the next cycle necessary for auto-ignition to occur.

The trapping of the exhaust of the previous cycle to sustain auto-ignition creates a cycle-to-cycle coupling in exhaust recompression HCCI affecting both the temperature and the composition of the charge. The dynamics of this coupling can vary dramatically at different operating points. Figure 1 shows open-loop data collected at early and late phasing respectively. In the upper diagram the exhaust valve was closed earlier which yielded a higher concentration of exhaust gases in the next cycle. The difference in variance between the operating points is evident.

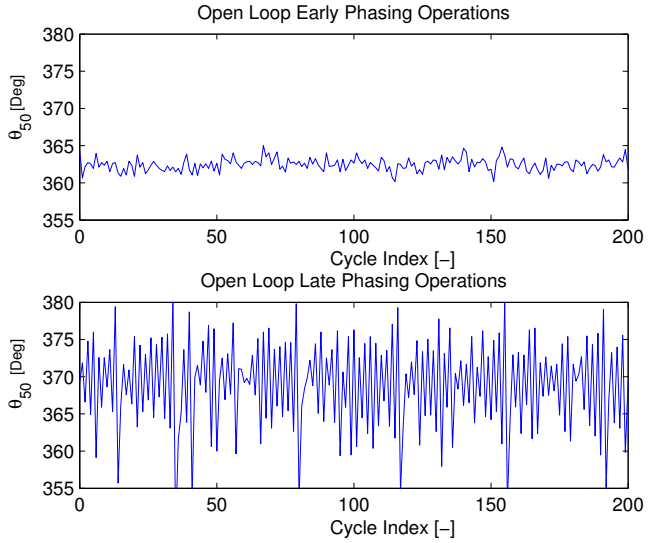

Fig. 1. Early phasing and late phasing operation (reproduced from [2]).

In [3], it was demonstrated that there were three qualitative types of temperature dynamics of exhaust recompression HCCI across a wide range of ignition phasing points; smooth decaying for early ignition phasing, oscillatory for late ignition phasing, and strongly converging for moderate phasing. As a result, the authors proposed a switching model consisting of three linear sub-models that captures the qualitative changes in dynamics. Using this switching linear model as a basis, this paper presents experimental results on control of the combustion phasing of recompression HCCI using a model predictive controller (MPC). MPC based on the switching linear model can be particularly useful for large step changes in ignition phasing. For example, in the case of transitioning from the early phasing point to the late, oscillatory, phasing point shown in Fig. 1, MPC has the advantage of anticipating the change in system dynamics and can issue appropriate control input o avoid undesirable transient behaviour.

Results on model predictive control of HCCI based on statistical models were presented in [4] and results using

A. Widd , P. Tunestål, and R. Johansson were supported by KCFP, Closed-Loop Combustion Control (Swedish Energy Adm: Project no. 22485-1), VinnPro (Project no. P32220-1), and LCCC, Swedish Research Council, Ref. VR 2007-8646. H.H. Liao and J.C. Gerdes would like to acknowledge General Motors Company and Robert Bosch LLC for their financial and technical support of this work.

A. Widd and R. Johansson are with the Department of Automatic Control, Lund University, Box 118 SE 221 00 Lund, Sweden. {anders.widd | rolf.johansson}@control.lth.se

H.H. Liao and J.C. Gerdes are with the Department of Mechanical Engineering, Stanford University, USA. {hhliao | gerdes}@stanford.edu

P. Tunestål is with the Division of Combustion Engines, Department of Energy Sciences, Lund University. per.tunestal@energy.lth.se

physical modeling in [5]. In [5], it was noted that the control performance was improved by changing linearization depeneding on operating point. A previous publication on hybrid model predictive engine control is [6], where the authors model a spark-ignited engine using separate models for homogeneous and stratified charge.

The work presented in this paper focuses on the dynamic response to set-point changes in the desired combustion phasing. A fast response to set-point changes with little overshoot can be critical to avoid misfire or too high peak pressures during transient operation. A switching linear quadratic controller and a hybrid model predictive controller were implemented and compared in simulation and experiments. Due to the limited computational capability of the experimental testbed, explicit versions of the model predictive controller were computed. As the results show, the two controller types performed similarly during smaller changes in set point and produced similar levels of output variance. However, during larger transients when a change in combustion phasing from around top dead center to a later phasing point was desired, the linear quadratic controller produced a large overshoot and subsequent oscillations. A sufficiently large overshoot could possibly lead to misfire, and in the case of exhaust recompression HCCI it can be difficult to recover from a single misfire as the charge temperature of the next cycle will be low.

The structure of the piecewise linear model is presented in Section II. The two control strategies are described in Section III as well as the controller-observer structure used. Implementational aspects are discussed in Section IV. Simulation results and experimental results are given in Section V, followed by a discussion in Section VI.

II. Modeling

A physics-based nonlinear model on the form (1) was presented in [7]. The system states, $[O_2]$ and T, denote the oxygen concentration in the cylinder and the charge temperature at 300 crank angle degrees (60 degrees before combustion top dead center). These thermodynamic states can be related to ignition timing through an Arrhenius integral [8]. Particularly, the charge temperature state has a dominant influence on combustion phasing. The crank angle where 50% of the energy in the injected fuel has been released, θ_{50}, is used as a proxy for ignition timing in this work and the control objective is to track a desired θ_{50} value. The control input V_{EVC} denotes the volume at the crank angle of exhaust valve closing, θ_{EVC}, and describes the amount of exhaust gases trapped in the cylinder. The model structure is on the following form, where $f_1(O_2(k), T(k), V_{\text{EVC}}(k))$, $f_2(O_2(k), T(k), V_{\text{EVC}}(k))$, and $g(O_2(k), T(k))$ are nonlinear functions:

$$O_2(k+1) = f_1(O_2(k), T(k), V_{\text{EVC}}(k)) \tag{1a}$$
$$T(k+1) = f_2(O_2(k), T(k), V_{\text{EVC}}(k)) \tag{1b}$$
$$\theta_{50}(k) = g(O_2(k), T(k)) \tag{1c}$$

A. Multiple Linearizations

Linearizations were obtained by numerically differentiating the functions in (1) around steady-state operating points. The linearizations were on the form

$$x(k+1) = A_i x(k) + B_i u(k) + d_i \tag{2a}$$
$$y(k) = C_i x(k) + e_i \tag{2b}$$

where

$$x(k) = \begin{bmatrix} O_2(k) \\ T(k) \end{bmatrix}, \quad u(k) = V_{\text{EVC}}(k) \tag{3}$$

and A_i, B_i, C_i, d_i, and e_i constitute the system dynamics at linearization point i. The constants d_i and e_i were added as the models were normalized around baseline steady-state values, so that a given value of the state vector or control signal has a one-to-one correspondence to physical values, see [3].

In [3], it was observed that there are three qualitative types of temperature dynamics of exhaust recompression HCCI. For higher charge temperatures, corresponding to early phasing operation, the temperature is smoothly converging to the steady-state value. When the charge temperature is low, corresponding to late phasing operation, the temperature is oscillating around the steady-state temperature between every cycle. The middle region, corresponding to moderate charge temperature, shows a considerably weaker cycle-to-cycle coupling of the temperature state. These three qualitative temperature dynamics manifest themselves in the linearizations of the nonlinear model about steady-state operating points, as seen in the respective A, B, and C matrices in (4)-(6). Note that the linearizations shown in (4)-(6) are associated with descending steady-state charge temperature.

1) Early phasing, higher charge temperature:

$$A_1 = \begin{bmatrix} 0.579 & 0.512 \\ -0.005 & 0.1268 \end{bmatrix} \quad B_1 = \begin{bmatrix} -2.254 \\ 0.524 \end{bmatrix}$$
$$C_1 = \begin{bmatrix} -0.015 & -0.435 \end{bmatrix} \tag{4}$$

2) Middle region, moderate charge temperature:

$$A_2 = \begin{bmatrix} 0.527 & 0.193 \\ -0.007 & -0.010 \end{bmatrix} \quad B_2 = \begin{bmatrix} -1.481 \\ 0.454 \end{bmatrix}$$
$$C_2 = \begin{bmatrix} -0.023 & -0.652 \end{bmatrix} \tag{5}$$

3) Late phasing, lower charge temperature:

$$A_3 = \begin{bmatrix} 0.493 & -0.247 \\ -0.011 & -0.313 \end{bmatrix} \quad B_3 = \begin{bmatrix} -1.219 \\ 0.423 \end{bmatrix}$$
$$C_3 = \begin{bmatrix} -0.036 & -1.031 \end{bmatrix} \tag{6}$$

The eigenvalues of each linearization are presented in Table I. The oscillating nature of the late phasing region is reflected in the eigenvalue in -0.3133 while the corresponding eigenvalue for early phasing region is located in 0.1325. The deadbeat dynamics of the middle region corresponds to the eigenvalue close to the origin.

TABLE I
EIGENVALUES FOR THE LINEARIZATIONS

Linearization	Eigenvalue 1	Eigenvalue 2
1 (Early phasing)	0.5733	0.1325
2 (Middle region)	0.5244	0.0016
3 (Late phasing)	0.4933	-0.3133

B. Piecewise Affine Representation

To approximate the change in the nonlinear system behavior, Liao et al. partitioned the state space into three regions and used one linearization on the form (2) to model the HCCI engine in each region [3]. In the description below, the number of regions is denoted by n, as there may be advantages to include more regions in order to improve model fidelity, while the experimental results where obtained using the three linearizations described in the previous section. Region i in the state space is defined by a pair of upper and lower temperature limits, $T_{i,u}$ and $T_{i,l}$. To be consistent with the descending steady state temperature of the linearized points in the previous section, it holds that $T_{i+1,u} = T_{i,l}$. Region i was active when $T_{i,l} < T(k) \leq T_{i,u}$. The resulting system takes the following form

$$\begin{aligned} x(k+1) &= A_i x(k) + B_i u(k) + d_i, \\ y(k) &= C_i x(k) + e_i, \end{aligned} \quad \text{if } \begin{bmatrix} x(k) \\ u(k) \end{bmatrix} \in \Omega_i \tag{7}$$

where

$$\Omega_i \triangleq \{x : S_i x \leq T_i\} \tag{8}$$

The matrices S_i and T_i define the region where model i is active. The threshold on the temperature state, the second element of $x(k)$, can be described by

$$S_i = \begin{bmatrix} 0 & 1 \\ 0 & -1 \end{bmatrix}, \quad T_i = \begin{bmatrix} T_{i,u} \\ -T_{i,l} \end{bmatrix}, \tag{9}$$

The model was implemented in the HYSDEL language, see [9], and the Hybrid Toolbox [10], was used to generate the model predictive controllers. The model was implemented by defining the states and outputs as sums of the dynamics of each region with a boolean weighting parameter, as suggested in [10].

III. CONTROL

A switched linear quadratic controller and a hybrid model predictive controller were implemented and compared in simulations and experiments. The control strategies are described in Sections III-B and III-C respectively. Both control strategies were combined with a switched state estimator based on output measurements.

A. State Estimation

Measurements of the combustion phasing were used to estimate the charge temperature and oxygen concentration in the cylinder. Let $x(k+j|k)$ denote the estimate of $x(k+j)$ given a measurement of the output $y(k)$. Given the current active region, i.e., the current value of i, the *measurement update* was performed according to

$$x(k|k) = (I - M_i C_i)x(k|k-1) + M_i(y(k) - e_i) \tag{10}$$

where M_i is the innovation gain for region i. The estimate $x(k|k)$ was used to calculate the control signal. Using the control signal for the next cycle, the *time update* was performed by calculating the system response using (7)-(8) to determine an estimate of the active region at the next cycle and setting

$$x(k+1|k) = A_i x(k|k) + B_i u(k) + d_i \tag{11}$$

B. Switched Linear Quadratic Control

A linear quadratic controller on the form

$$u(k) = -Kx(k) \tag{12}$$

was obtained for each region by minimizing the following cost function

$$J(u) = \sum_{j=0}^{\infty} ||Q_y y(j)||_2 + ||Q_u u(j)||_2 \tag{13}$$

where the matrices Q_y and Q_u define the penalties on output deviations and control usage respectively and $||\cdot||_2$ indicates the 2-norm. Reference tracking was introduced by feedforward, so that the full control law took the form

$$u(k) = N_u y_r(k) + K(N_x y_r(k) - x(k)) \tag{14}$$

The feedforward gains N_u and N_x were determined by checking which region that would be active at the requested reference value $y_r(k)$ while the feedback gain K was chosen as that corresponding to the current active model region.

C. Hybrid Model Predictive Control

The control strategy is composed of solving a finite horizon optimal control problem at each sample and applying the first step of the resulting control sequence. At the next sample, the procedure is repeated with the current state estimate as initial condition in the optimization problem. Since no constraints were considered, the optimal control problem to be solved at cycle k was

$$\begin{aligned} &\min \textstyle\sum_{j=k}^{k+N} ||Q_y \left(y(j|k) - y_r(j)\right)||_2 + ||Q_u u(j)||_2 \\ &\text{subject to Eqs. } (7), (8) \end{aligned} \tag{15}$$

The weights Q_y and Q_u were the same as those used when designing the LQ controller and N defined the length of the prediction horizon.

IV. EXPERIMENTAL IMPLEMENTATION

This section describes the implementation of the model predictive controller and the experimental conditions.

A. Controller Implementation

The data acquisition and control system was implemented using xPC target [11]. The sample time was 0.1 ms in order to get a good reading of the pressure trace while the controller commands were executed once per engine cycle. As there is a certain overhead connected with data acquisition, signal processing, and control actuation, the actual computation time available to obtain the next control signal was considerably smaller.

1) Explicit Model Predictive Control: To reduce the online computational demand, an explicit representation of the hybrid model predictive controller was computed, denoted EMPC in the following. The control action was then given by

$$u(k) = F_i \begin{bmatrix} x(k) \\ r(k) \end{bmatrix} + g_i, \text{ for } \begin{bmatrix} x(k) \\ r(k) \end{bmatrix} \in \zeta_i \qquad (16)$$

where ζ_i defines controller partition i, and $\cup_i \zeta_i$ is the set of states and references for which a feasible solution to the original MPC problem exists, see [12], [10]. Note that the controller partitions of (16) have the form

$$\zeta_i = \left\{ \begin{bmatrix} x \\ r \end{bmatrix} : H_i \begin{bmatrix} x \\ r \end{bmatrix} \leq R_i \right\} \qquad (17)$$

and are distinct from the model regions of (7).

To satisfy computational constraints, the number of partitions can be decreased by reducing the prediction horizon N or by removing partitions based on size. Using the Hybrid Toolbox [10], this can be achieved by removing any partitions whose Chebychev radius is smaller than a given tolerance ρ_f. During tests, it was possible to run controllers with more than 60 partitions on the engine control computer with a 3.2 GHz Intel Pentium 4 processor. The results in Sec. V were obtained with a controller with 21 partitions, obtained with $N = 2$ and $\rho_f = 10^{-6}$.

B. Experimental Platform

A 2.2-liter 4-cylinder General Motors Ecotech gasoline engine with direct fuel injection was used in the experiments. The engine was equipped with a variable valve actuation (VVA) system described in [13]. The system allowed for independent cycle-to-cycle control of both intake and exhaust valve timings. In this study, however, only the exhaust valve was used as a control input. The intake valve was closed 30 crank angle degrees after bottom dead center and all valve events had a duration of 140 crank angle degrees. Three of the cylinders were operated with switching state feedback controllers in all tests while cylinder 4 was operated with either an EMPC or an LQ controller. All presented experimental results were obtained from this cylinder.

V. Results

This section presents numerical results obtained by simulating the nonlinear model in Eq. (1) followed by experimental results obtained on the engine.

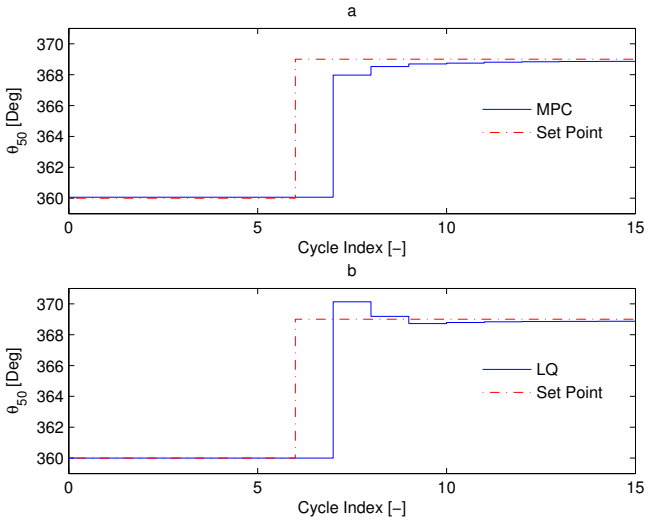

Fig. 2. Simulated combustion phasing during a set point change using MPC (a) and LQ (b) controllers.

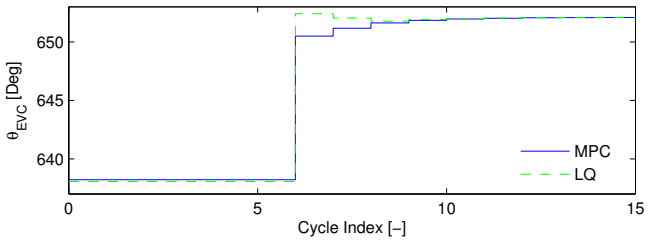

Fig. 3. Simulated control signals for the MPC and LQ controllers corresponding to Fig. 2.

A. Numerical Results

To see the benefits of predicting across model regions, the nonlinear model (1) was simulated with the switched LQ controller and the MPC. The result when making a step change in desired phasing from top dead center to 9 degrees after top dead center (ATDC) is shown in Fig. 2 and the corresponding control signals are shown in Fig. 3. The LQ controller produces a slight overshoot whereas the MPC shows a smoother convergence to the later set point. There were very minor differences between the two controllers during smaller set point changes.

B. Experimental Results

Figures 4 and 5 show characteristic outputs and control signals of the LQ and EMPC in experiments. The desired θ_{50} was changed from 2 degrees ATDC to 9 degrees ATDC. The LQ controller produced a considerable overshoot during the step compared to the EMPC. The steady-state behavior of the two controllers was very similar. Comparing with Fig. 2, the overshoot and subsequent variations with the LQ controller were worse than the simulation results implied. The qualitative behavior in terms of the difference between the two control approaches was similar but the results suggest that the control model understates the lack of damping around the later set point.

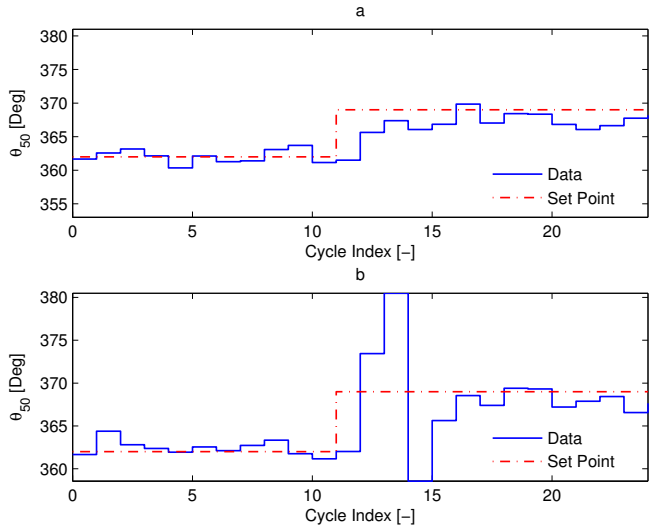

Fig. 4. Experimental verification of combustion phasing during a set point change using EMPC (a) and LQ (b) control.

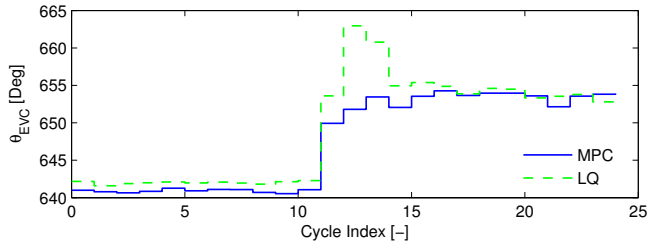

Fig. 5. Experimental verification of control signals for the EMPC and LQ controllers corresponding to Fig. 4.

Figures 6 and 7 show the combustion phasing and control signal for the EMPC and LQ controllers during a sequence of step changes in the desired combustion phasing. The steady-state output variance was comparable between the two around all set-points. Compared to the open-loop behavior in the lower plot in Fig. 1, both controllers improved steady state performance considerably in terms of peak-to-peak variance. The EMPC produced some chatter in the control signal around the middle set points 364 and 367 which increased the output variance slightly compared to the LQ controller.

VI. Discussion

In Fig. 7 (a) it is apparent that some chattering occurs in the control signal around the middle operating points. Fig. 8 shows the corresponding temperature estimate along with the upper and lower thresholds for model region 2. During the chattering, the temperature estimate is switching between model region 1 and 2 or between model region 3 and 2. A possible explanation for the chattering behavior of the controller is that the model in region 2 suggests a substantially weaker cycle-to-cycle dependence of the charge temperature than the other regions, which should promote larger control signal changes.

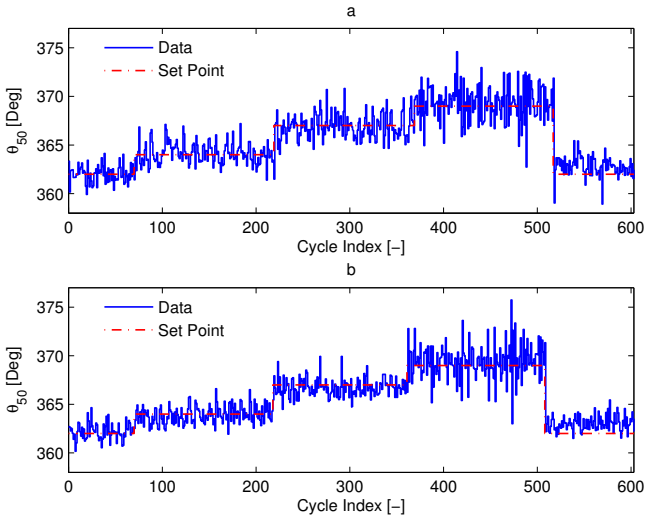

Fig. 6. Combustion phasing during a series of set point changes using EMPC (a) and LQ (b) controllers.

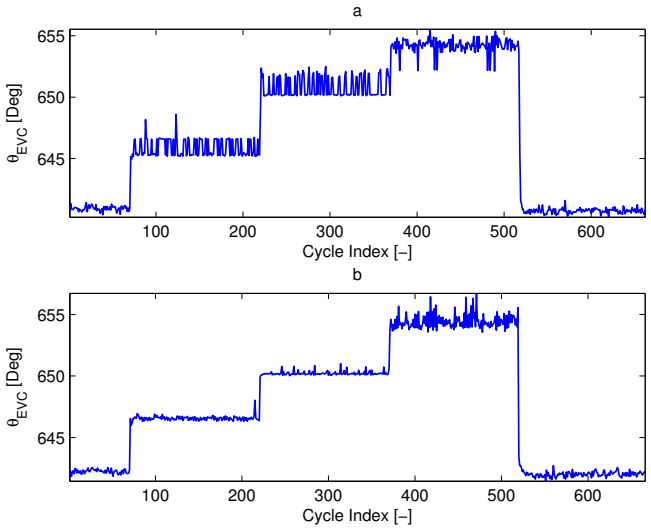

Fig. 7. Control signal corresponding to Fig. 6 using EMPC (a) and LQ (b) controllers.

A possible modification to the control structure to attenuate this behavior would be to include a hysteresis band around the temperature threshold between two neighboring model regions. In effect this means that the temperature estimate needs to be sufficiently far into a neighboring region before switching region. This would not affect the performance across multiple regions presented in Figs. 4-5. A possible hysteresis scheme for region 1 would be

$$i(k)=1 \text{ when } \begin{cases} i(k-1)=1 & \text{and } T(k) > T_{1,l} - h_{1,2} \\ i(k-1)=2 & \text{and } T(k) > T_{1,l} + h_{2,1} \\ i(k-1)=3 & \text{and } T(k) > T_{1,l} \end{cases} \tag{18}$$

where $h_{1,2}$ and $h_{2,1}$ modify the thresholds for passing from region 1 to region 2 and vice versa. When $h_{1,2} = h_{2,1} = 0$, the nominal thresholds are obtained. The condition for

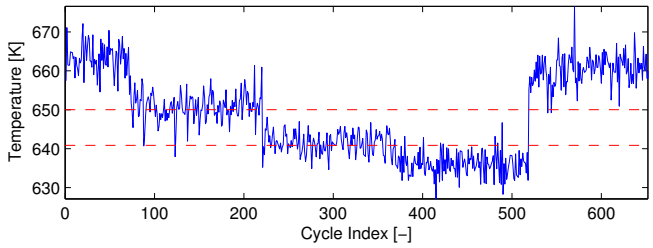

Fig. 8. Temperature estimate and temperature thresholds (dashed) corresponding to the experimental results in Fig. 6.

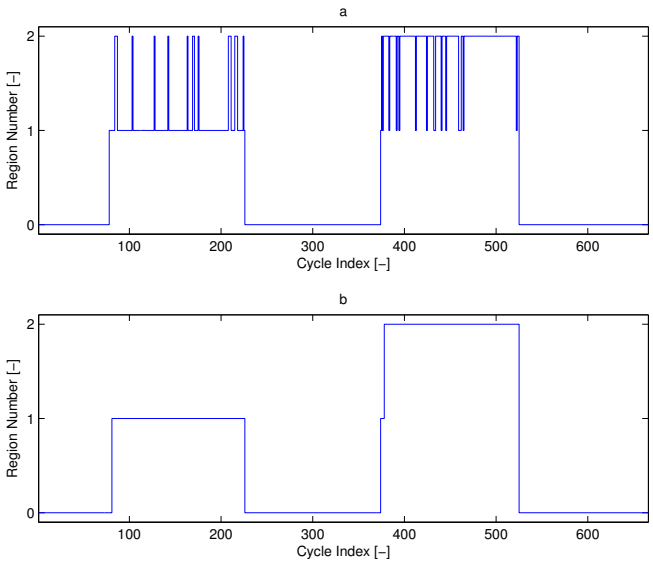

Fig. 9. Region estimate using the original PWA formulation (a) and with hysteresis added (b) corresponding to Fig. 8.

transitioning from region 3 to region 1 is left unchanged from the representation in Eqs. (7)-(8). The transition rules for regions 2 and 3 would follow the same principle. Figure 9 shows the active region estimate using the original PWA model formulation and that with hysteresis added. The hysteresis band was set to approximately 4 degrees around each threshold, which was sufficient to remove the chattering in the region estimate.

The explicit MPC that was used for generating the results consisted of 21 partitions. During tests it was possible to run controllers with more than 60 partitions, suggesting that it might be possible to increase the complexity of the controller by adding constraints to relevant variables or introducing the hysteresis bands without exceeding the computational limitations of the hardware used in this study.

The ability to predict across model region improved control performance when making large steps from an early phasing to a late phasing set point. The qualitative improvement was captured well in the simulation preceeding the experiments although the actual experimental results exhibited larger overshoot and subsequent transient behavior when using the LQ controller. Comparing the simulation results and the experimental results suggests that the nonlinear model understates the lack of damping in the late phasing region. A possible explanation for the overshoot in the LQ case is that only the feedforward part of the LQ implementation accounts for changing model regions while the feedback part uses the gains of the current region. The MPC, on the other hand, accounts for the future change in model region and produces a smaller initial change in the control signal followed by a smoother transient.

VII. Conclusion

Hybrid MPC was implemented to control the combustion phasing of exhaust recompression HCCI and compared to a switched LQ controller. The controllers were based on a piecewise affine model constructed from linearizations of a physics-based nonlinear model. The qualitative behavior of the controllers could be observed both in simulation and in experiments. To reduce the computational requirements of experimental evaluation, the explicit form of the MPC was calculated. The ability to predict across model region changes resulted in a smoother transient with no overshoot when traversing several model regions.

References

[1] J. Bengtsson, P. Strandh, R. Johansson, P. Tunestål, and B. Johansson, "Hybrid modelling of homogeneous charge compression ignition (HCCI) engine dynamic—A survey," *Int. J. of Control*, vol. 80, no. 11, pp. 1814–1848, Nov. 2007.

[2] H.-H. Liao, N. Ravi, A. F. Jungkunz, A. Widd, and J. C. Gerdes, "Controlling combustion phasing of recompression HCCI with a switching controller," in *Proc. Fifth IFAC Symp. on Advances in Automotive Control*, Munich, Germany, July 2010.

[3] H.-H. Liao, N. Ravi, A. F. Jungkunz, J.-M. Kang, and J. C. Gerdes, "Representing change in HCCI dynamics with a switching linear model," in *2010 American Control Conf. (ACC 2010)*, Baltimore, Maryland, USA, 2010.

[4] J. Bengtsson, "Closed-loop control of HCCI engine dynamics," Ph.D. dissertation, Dept. of Automatic Control, Lund Institute of Technology, Lund University, Sweden, Nov. 2004.

[5] A. Widd, "Predictive control of hcci engines using physical models," Department of Automatic Control, Lund University, Sweden, Licentiate Thesis TFRT--3246--SE, May 2009.

[6] N. Giorgetti, G. Ripaccioli, A. Bemporad, I. Kolmanovsky, and D. Hrovat, "Hybrid model predictive control of direct injection stratified charge engines," *Mechatronics, IEEE/ASME Transactions on*, vol. 11, no. 5, pp. 499–506, Oct. 2006.

[7] N. Ravi, M. J. Roelle, A. F. Jungkunz, and J. C. Gerdes, "A physically based two-state model for controlling exhaust recompression HCCI in gasoline engines," in *Proc. of IMECE'06*, Chicago, Illinois, USA, Nov. 2006.

[8] G. M. Shaver, J. C. Gerdes, and M. Roelle, "Physics-based closed-loop control of phasing, peak pressure and work output in HCCI engines utilizing variable valve actuation," in *Proc. 2004 American Control Conf. (ACC 2004)*, Boston, MA, USA, June 2004.

[9] D. Jost and F. Torrisi, "HYSDEL - Programmer Manual," Tech. Rep., Aug. 2002, http://control.ee.ethz.ch/index.cgi?page= publications;action=details;id=799.

[10] A. Bemporad, "Hybrid Toolbox - User's Guide," 2004, http://www.dii.unisi.it/hybrid/toolbox.

[11] Mathworks, "xPC Target 4 - User's Guide," The Mathworks inc., 2010.

[12] A. Bemporad, F. Borrelli, and M. Morari, "Optimal controllers for hybrid systems: Stability and piecewise linear explicit form," in *39th IEEE Conf. on Decision and Control*, Sydney, Australia, Dec. 2000, pp. 1810–1815.

[13] H.-H. Liao, M. J. Roelle, and J. C. Gerdes, "Repetitive control of an electro-hydraulic engine valve system," in *2008 American Control Conf. (ACC 2008)*, Seattle, Washington, USA, 2008.